PROCESSING TECHNOLOGY OF FGMMCS FROM THE AA6060/TiB_2 SYSTEM BY CENTRIFUGAL CASTING

Constantin Domenic STĂNCEL[1]*, Nicolae CONSTANTIN[2], Mihai BUȚU[3], Georgiana CHIȘIU[4], Florentina NICULESCU[5], Larisa BUȚU[6], Sebastian Titus DUMA[7], Marinela MARINESCU[8]

In order to obtain a continuous gradient structure with a reinforced exterior of heavier TiB_2 particles in an aluminium metal matrix composite obtained via the in-situ process, we used the centrifugal casting route. This paper describes the preparation method and offers an overview of the technologies used to process the AA6060/TiB_2 FGMMCs. Using electron microscopy with EDS, optical microscopy, diffraction, DLS, we highlighted the morphology and distribution of TiB_2 particles in the obtained layers. Tests have been performed on FGMMCs for the determination of abrasive wear, thus determining the Archard coefficient.

Keywords: FGMMCs, technology, Archard coefficient, FGMs, abrasive wear, titanium diboride (TiB_2)

1. Introduction

Due to their superior mechanical properties and unique physical characteristics, such as low thermal expansion coefficients, metallic matrix composites are attractive for many industrial applications, such as aerospace, maritime, automotive, rail, construction, packaging, electricity distribution, various sports and leisure equipment.

[1] Faculty of Materials Science and Engineering, University POLITEHNICA of Bucharest, Romania, e-mail: stancel.constantin@yahoo.com
[2] *. Faculty of Materials Science and Engineering, University POLITEHNICA of Bucharest, Romania, e-mail: nctin2014@yahoo.com
[3] Faculty of Materials Science and Engineering, University POLITEHNICA of Bucharest, Romania, e-mail: mihaibutu@yahoo.com
[4] Faculty of Mechanics, University POLITEHNICA of Bucharest, Romania, e-mail: georgiana_bosoi@yahoo.com
[5] Faculty of Materials Science and Engineering, University POLITEHNICA of Bucharest, Romania, e-mail: flori.pereteanu@yahoo.com
[6] Faculty of Industrial and Robotic Engineering, University POLITEHNICA of Bucharest, Romania, e-mail: l_butu@yahoo.com
[7] Faculty of Mechanics, University POLITEHNICA of Timisoara, Romania, corresponding author e-mail: sebastian.duma@upt.com
[8] Faculty of Industrial and Robotic Engineering, University POLITEHNICA of Bucharest, Romania, e-mail: m_marinescuro@yahoo.com

Metal matrix composites are mostly used due to improved mechanical properties, such as high-temperature resistance, wear resistance, improved ductility and electrical conductivity.

Most metals and alloys could be used as matrices, which require reinforcing materials, which must be stable in a certain temperature range and non-reactive. However, in practice, the alternatives for low-temperature applications are not very many.

Over the years, aluminium–matrix composites have been used in numerous structural, non-structural and functional applications in different engineering sectors [1]. Driving force for the utilization of aluminium–matrix composites in these sectors includes performance, economic and environmental benefits [1]. The key benefits of aluminium based MMCs composites in the transportation sector are lower fuel consumption, less noise and lower airborne emissions [2].

Aluminium composites reinforced with hard ceramic particles have become increasingly attractive for research in the field of structural composites. Adding ceramic particles, such as TiB_2, SiC, Al_2O_3, B_4C, to an aluminium matrix does not significantly alter the material density, but instead, it leads to a significant increase in the specific strength and modulus of the composite [3].

There is a substantial difference between a functionally graded material and traditional composite material (MMC). MMCs are a class of advanced materials, consisting of one or more materials combined in solid states with distinct physical and chemical properties [4].

The variation of the properties in an FGM reduces the thermal stresses, the residual stresses and the stress concentrations found in the traditional composites. FGMs may include more than two constituent phases [4].

Gradient materials offer the possibility to combine two materials properties avoiding most of the disadvantages of a bimaterial [5]. In contrast, traditional composites are homogeneous mixtures, and they, therefore, involve a compromise between the desirable properties of the component materials [5]. Since significant proportions of an FGM contain the pure form of each component, the need for compromise is eliminated. The properties of both components can be fully utilized. For example, the toughness of metal can be associated with the refractoriness of a ceramic, without any compromise in the toughness of the metal side or the refractoriness of the ceramic side [5].

Functionally Graded Materials (FGMs) may be characterized by the variation in composition and structure gradually over volume, resulting in corresponding changes in the properties of the material [6]. The materials can be designed for specific function and applications.

FGMs were initially designed as thermal barrier materials for aerospace structural applications and fusion reactors [7].

Materials with a functional gradient eliminate the discontinuous interfaces existing in the composite material, where structural defects are triggered [8]. It replaces the discontinuous interface with a gradient interface that produces a smooth transition from one material to another [9].

A unique feature of FGMs is the ability to customize a material for a specific application [10].

Types of FGMs

At the beginning of the development of FGMs, the concept was to remove the discontinuous interface that existed in the traditional composite material and to replace it with the gradually changing interface, which was transformed into the changing chemical composition of this composite at this interface area.

The growing interest in this type of material has led to the development of different types of FGMs. The type of intended application determines the type of FGM which can be used.

The different types of materials with a functional gradient that are produced now are those formed by chemical composition gradient, porosity gradient and microstructural gradient. Each of these types of FGM is discussed in detail in the following sections.

The manufacturing process of an FGM can usually be divided into two steps. The initial one is building up of the spatially inhomogeneous structure called “gradation”. Another is the transformation of this structure into a bulk material called “consolidation”. In detail, the gradation process can be categorized into constitutive, homogenizing and segregating processes [11]. The grading processes can be classified into constituent, homogenization and segregation processes. The constituent processes are based on a gradual construction of the graded structure with powders [12]. In homogenization processes, a discontinuous interface between two materials is transformed into a gradient by transporting the material. The processes of homogenization and separation produce continuous gradients, but they have limitations regarding the types of gradients that can be produced. Usually, drying and sintering or solidification follow the grading step. These consolidation processes must be adapted for materials with a functional gradient: the processing conditions should be chosen so that the gradient is not destroyed or altered in an uncontrolled manner [11].

Chemical vapour deposition technique (CVD)

The chemical vapour deposition method is used to deposit functionally graded surface coatings and it gives excellent microstructure, but it can only be used for depositing thin surface coating. This method is energy-intensive and produces poisonous gases as their by-products [13].

Powder metallurgy

Powder metallurgy (PM) is commonly utilized in the industry in order to deliver practically graded material via the following three steps: weighing and blending of powder as indicated by the pre-composed spatial distribution as dictated by the functional prerequisite, stacking and ramming of the premixed-powders, sintering [14].

Centrifugal method

The centrifugal method is similar to the centrifugal casting, where the centrifugal force is used by rotating the mould to form the material with a crude functional gradient [15]. Material with a functional gradient is produced in this way because of the difference between the densities of the materials and the rotation of the mould. Although continuous grading can be achieved by the centrifugal method, only cylindrical shapes can be formed. [16] Another problem of the centrifugal method is that there is a limit on the type of gradient that can be produced because the gradient is formed by a natural process (centrifugal force and density difference) [13].

2. Experimental

TiB_2 nanoparticles [17] and microparticles were obtained in an electric furnace with KANTHAL resistance and graphite crucible, through the aluminothermic process between the molten aluminium alloy and the KBF_4 + K_2TiF_6 + Na_3AlF_6 salt mixture, at 750 – 950^{o}C. Potassium hexafluorotitanate (K_2TiF_6 with melting temperature 780°C and molecular weight 240.09 g/mol) and potassium tetrafluoroborate (KBF_4 with melting temperature 530°C and molecular weight 125.91g / mol) were used to obtain in-situ TiB_2 particles, and to protect the metal bath and dissolute the formed oxides, cryolite has been used (Na_3AlF_6 with melting temperature 1027°C and molecular weight 209.94g / mol).

In the process proposed in the paper, TiB_2 particles are formed by the aluminothermic reduction of hexafluorotitanate (K_2TiF_6) and tetrafluoroborate (KBF_4) with liquid aluminium:

$$3K_2TiF_6 + 6KBF_4 + 10Al = 3TiB_2 + 12KF + 10AlF_3 \quad (1)$$

To highlight the mechanism and kinetics of boron particle formation in aluminium alloys, 3 batch compositions were used for the 6060 alloys in order to obtain different concentrations of titanium diboride – 20%, 10% and 5% respectively. Fig. 1 shows the overall design of the installation used for obtaining the TiB_2-reinforced composite components through centrifugal solidification as well as the mould. Starting from the optimised parameters for obtaining the materials with aluminium base and reinforcing elements with TiB_2 particles, we

achieved, through centrifugal solidification, composite materials with different concentrations of particles in layers (
Table *1*). The particles were obtained by solubilizing the composites in concentrated hydrochloric acid and washing the resulting powder.

Table 1.

Studied composites

Composition of the material	Notation	Stirring time, min	Starting temperature for the solidification of the composite, ºC	Observations
200g 6060 alloy + 145g KBF_4 + 138g K_2TiF_6	A	2	660	High particle density
200g 6060 alloy + 73g KBF_4 + 69g K_2TiF_6	B	1.5	660	Low particle density
200g 6060 alloy + 40g KBF_4 + 40g K_2TiF_6	C	1	660	Low particle density

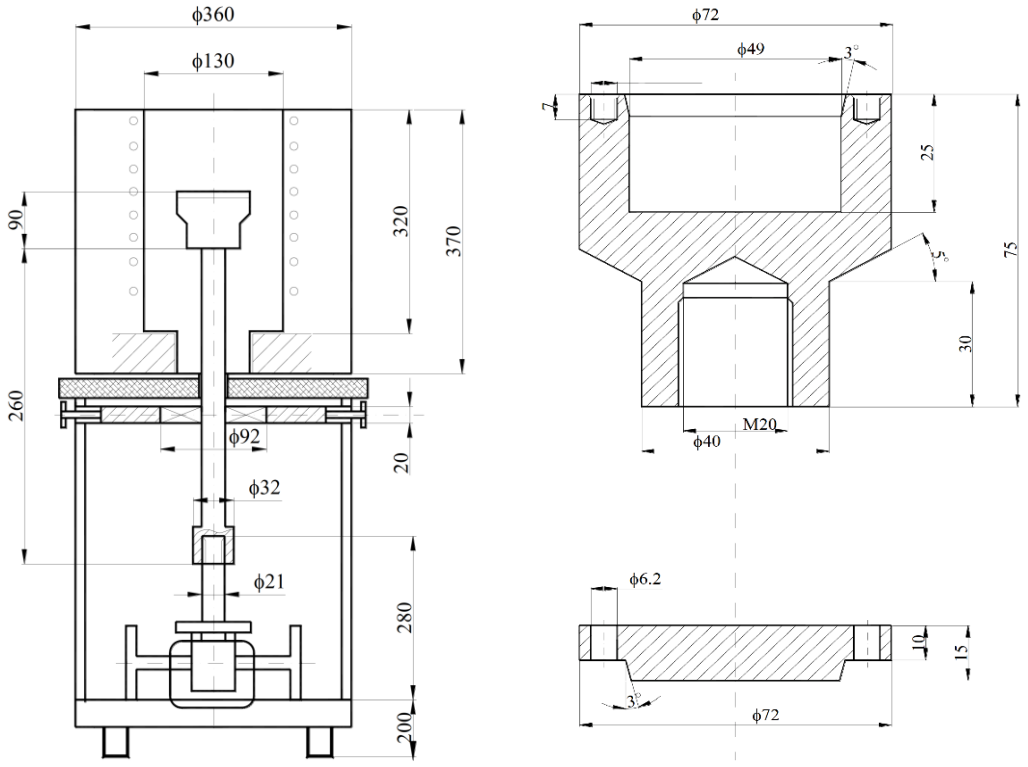

Fig. 1. The overall drawing of the installation used for the centrifugal solidification of the components to the left and the mould with the lid on the right

It is important to mention that whilst elaborating the TiB_2 functionally graded metal matrix composites (FGMMCs), using 1-2 minutes of stirring time and 15 – 20 minutes of reaction time in order to separate the resulting molten salts

from the melt, the resulting ceramic particles had dimensions of approximately 500 nm in diameter as shown in Fig. 2. The dimensional analysis of the TiB_2 particles was performed using Zetasizer Nano ZS analyser from Malvern.

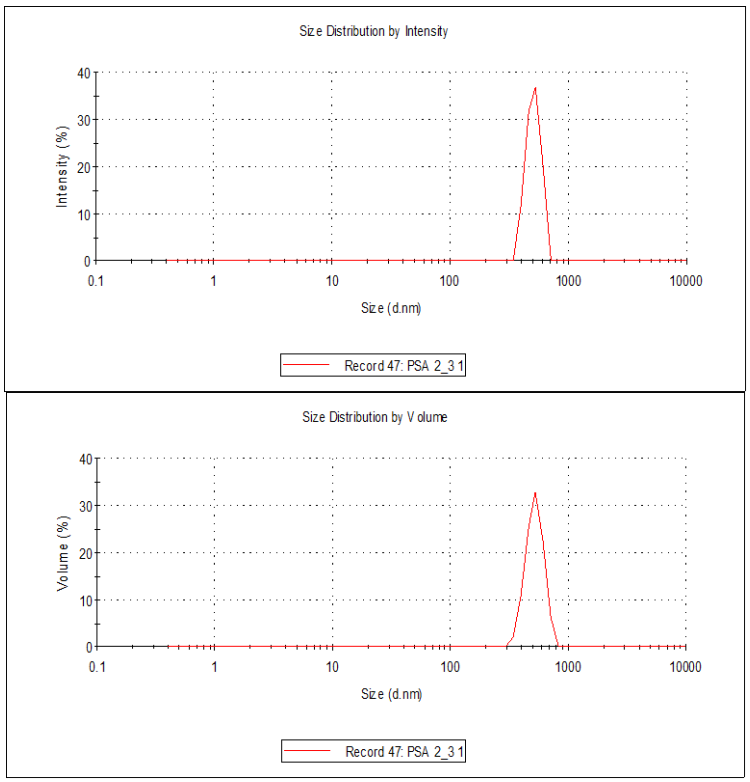

Size	Intensity
d.nm	%
396.1	11.7
458.7	31.8
531.2	36.8
615.1	19.7

Dimensional analysis of TiB_2 dispersed particles

D_{med} = 508.8 nm
20 minutes

Fig. 2. Particle size analysis of sample A

3. Results and discussions

As a result of the experiments, cylindrical samples with dimensions of ϕ50 mm and height of 50 mm were obtained, which later were cut down into rings with the height of 5 mm. From the materials obtained, samples were analysed through optical macro and microstructure (Fig. 3), layer analysis (Fig. 4), electron microscopy and EDS (Fig. 5) and XRD (Fig. 6).

Microstructural analysis by electron microscopy was performed on an SEM FEI Quanta Inspect F microscope, with field emission and equipped with an energy dispersive analysis system (EDS). The microstructure, phase analysis and the diameter of the imprint from the samples were measured directly using the Olympus UC30 camera and processed using the Olympus Stream image processing software.

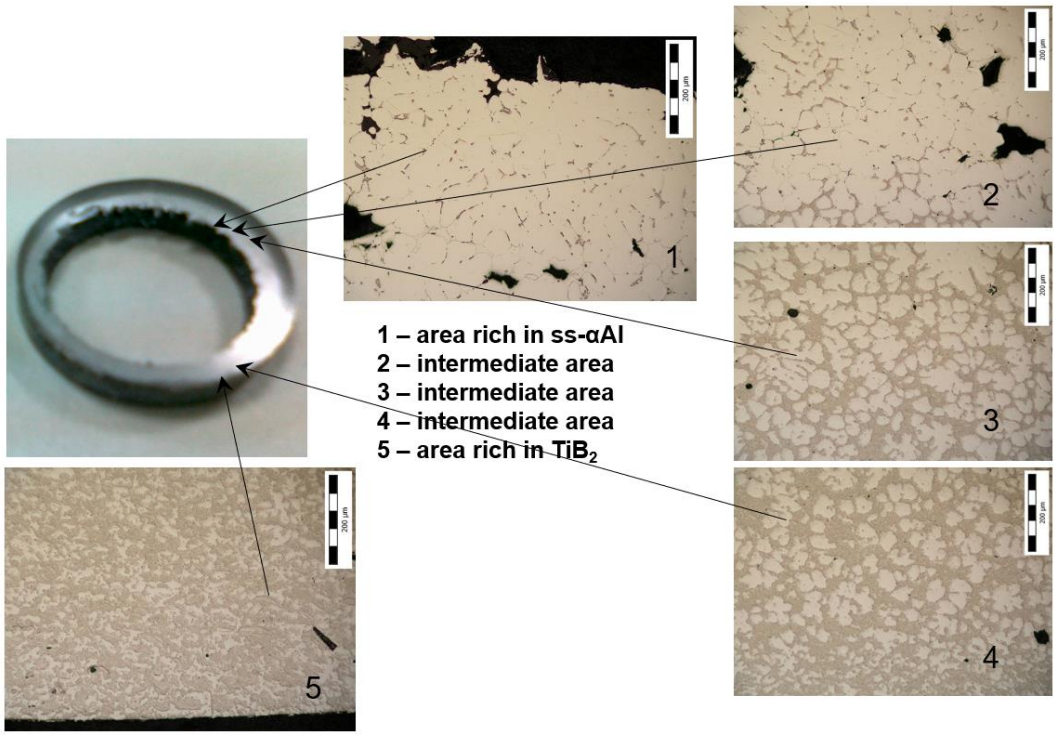

Fig. 3. Composite A macrostructure and microstructure

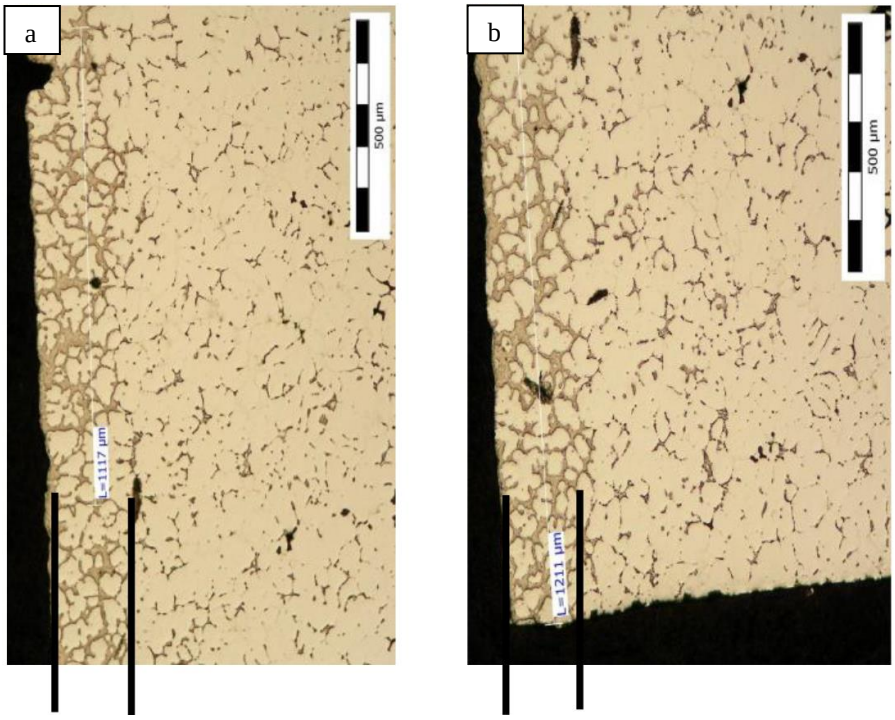

Fig. 4. Composite A layer analysis, (a) 1117 µm, (b) 1211 µm

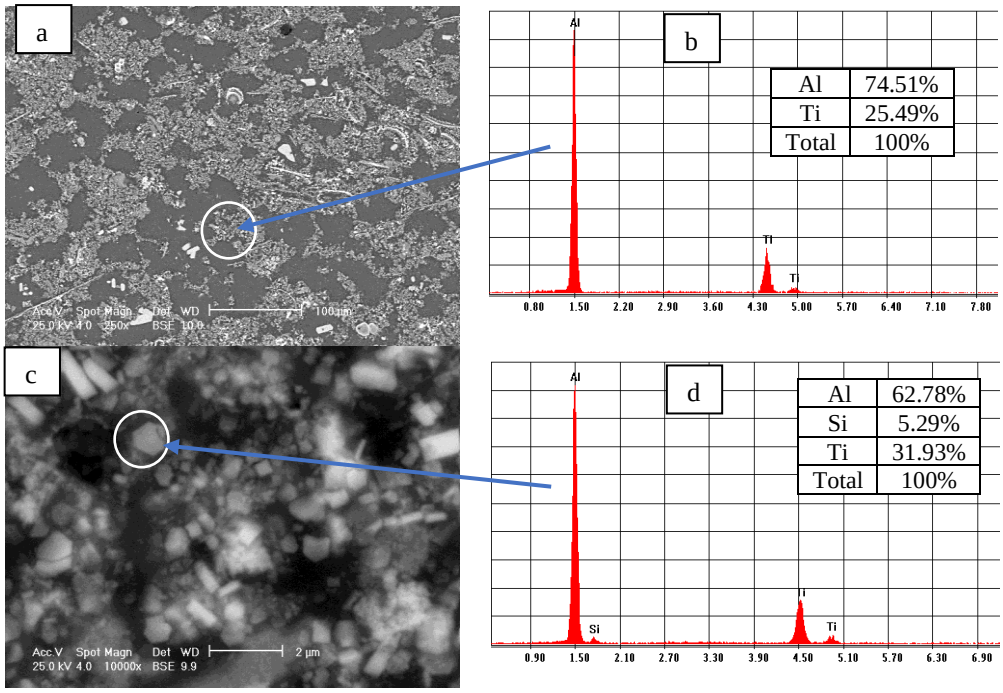

Fig. 5. Electronic microscopy (a and c) and EDS analysis, b) for small agglomerated grey compounds, d) for larger grey polyhedral compounds – composite A

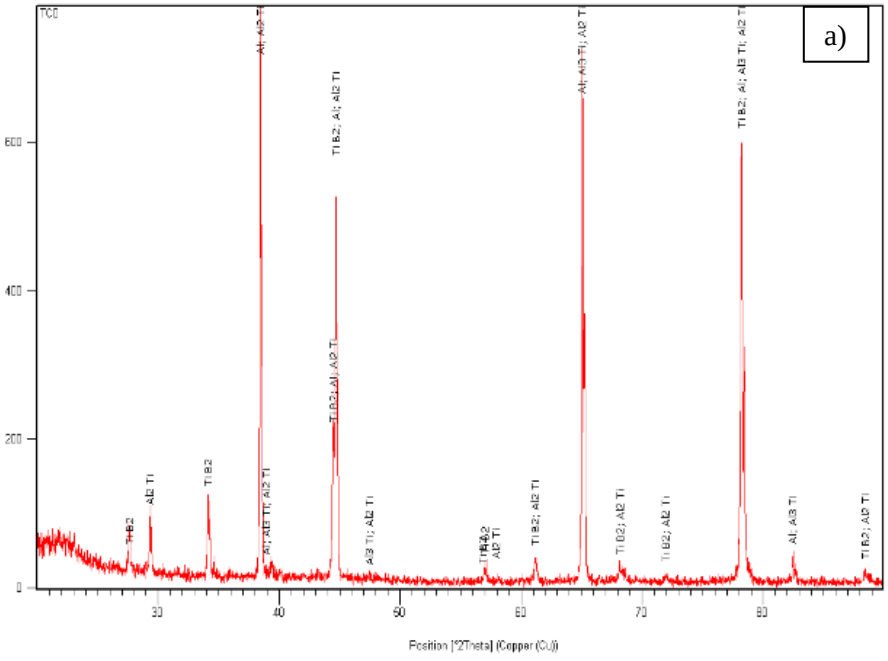

b)

No.	Visible	Ref. Code	Compound N...	Chemical Formula	Score	Scale ...	SemiQua
1	☐	01-075-1045	titanium boride	Ti B2	66	0.231	25
2	☐	01-071-4624	Aluminum	Al	48	0.670	67
3	☐	03-065-5174	Aluminum Ti...	Al3 Ti	3	0.081	7
4	☐	01-072-8513	Aluminum Ti...	Al2 Ti	0	0.017	1

c)

Element/compound	Crystallite size
Al	38.7 nm
TiB_2	28.9 nm
$TiAl_3$	2510.5 nm
$TiAl_2$	1825.8 nm

Fig. 6. Layer diffractogram (a) with high TiB_2 content, compositional analysis (b) and crystallite size (c) – composite A

The average crystallite dimensions were determined by using the Debye-Scherrer formula:

$$L = \frac{K\lambda}{\beta \cdot \cos\theta} \tag{2}$$

where λ is the X-ray wavelength in nanometer (nm), β is the peak width of the diffraction peak profile at half maximum height resulting from small crystallite size in radians and K is a constant related to crystallite shape, normally taken as 0.9. The value of β in 2θ axis of diffraction profile must be in radians. The θ can be in degrees or radians since the cosθ corresponds to the same number [18].

From the obtained materials samples were taken to determine the abrasive wear in order to determine the Archard coefficient (Fig. 7 – 9).

Table 2.

Materials used to determine the wear resistance

Material	Notation	The concentration of reinforcement elements	Imprint diameter
Composite A – uniform	A1	20%	0.39
Composite B – uniform	B1	13%	0.79
Composite C – uniform	C1	3%	0.33

A1, B1, C1 are composites with a homogeneous distribution of TiB_2 particles.

Composites A, B and C were used to obtain FGMMCs using the installation described in s 1. Materials with different concentrations of TiB_2 particles were obtained per layer depth. Samples were taken to highlight the concentration of reinforcing elements; the images were taken with the Olympus UC30 camera and were processed with the Olympus Stream software (phase analysis).

The resulting samples were subjected to an abrasive wear test using the CSEM CALOWEAR installation. The diameters of the imprint left following the wear test were determined by optical microscopy using the same Olympus UC30 (Figs. 7 – 9). The measurement principle of the equipment is based on a rotating sphere made of bearing steel, with a diameter d = 25 mm, that presses the surface with a certain load (F_N) [19].

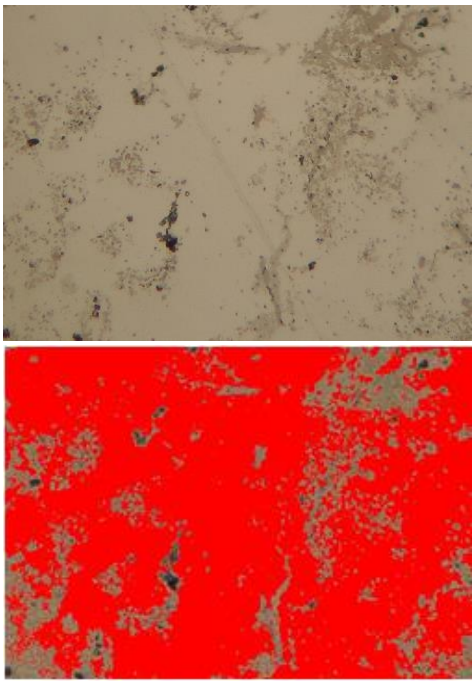

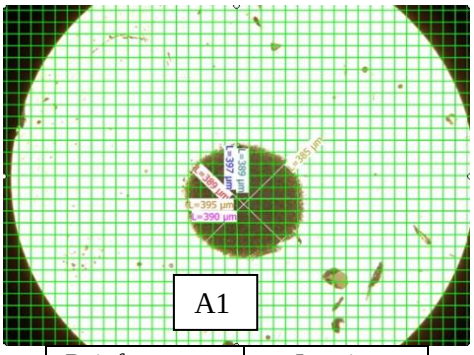

Reinforcement element	Imprint diameter
20%	0.39 mm

Fig. 7. Microstructure, phase analysis and the diameter of the imprint to the wear test – composite A1

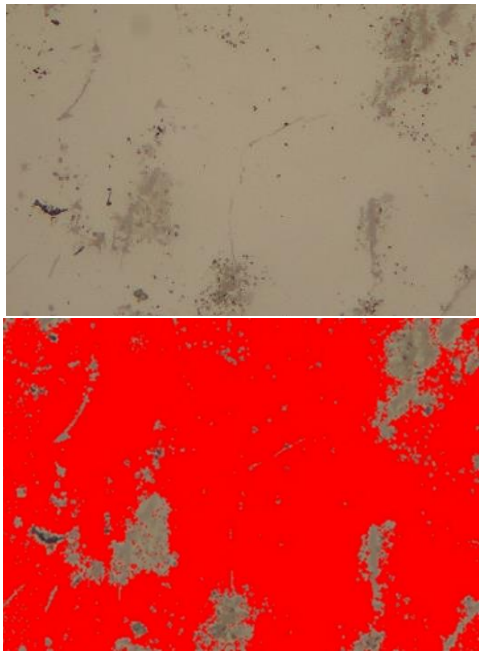

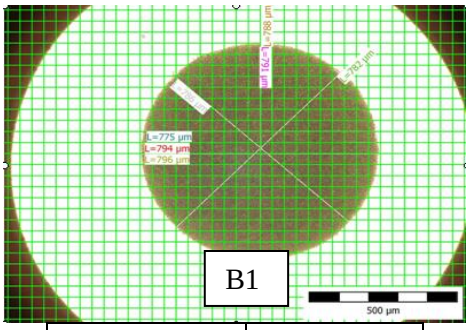

Reinforcement element	Imprint diameter
13%	0.79 mm

Fig. 8. Microstructure, phase analysis and the diameter of the imprint to the wear test – composite B1

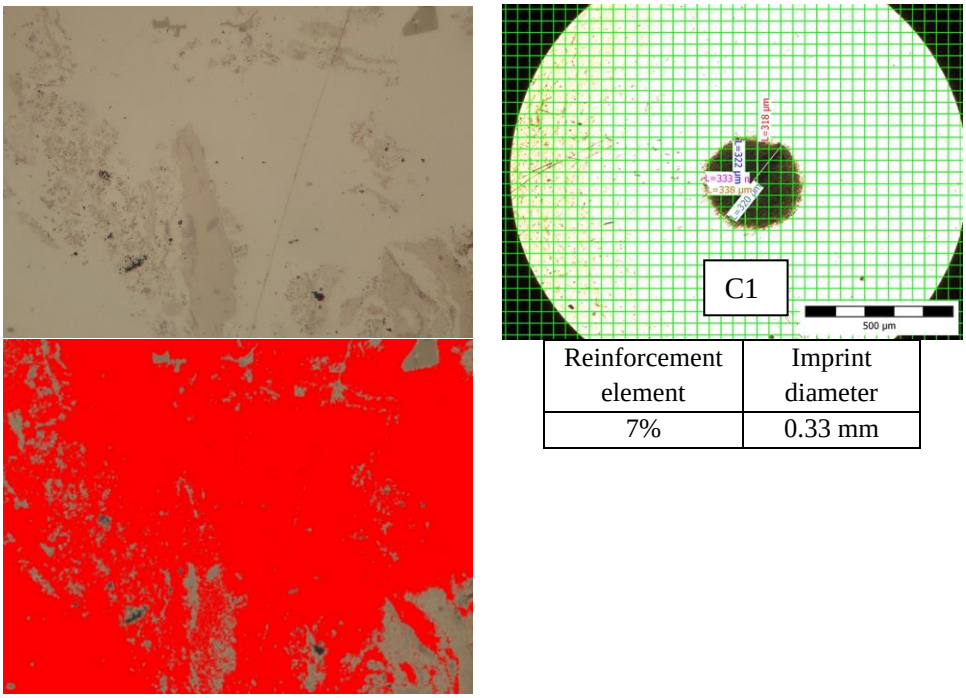

Reinforcement element	Imprint diameter
7%	0.33 mm

Fig. 9. Microstructure, phase analysis and the diameter of the imprint to the wear test – composite C1

Table 3.

Measured and calculated values for the determination of the Archard coefficient

Notation	Time [s]	Force press [N]	Shaft cycles no.	Ball cycles no.	Sliding dist. (m)	Imprint diameter (mm)	Crater (m)	Removed volume(m^3)
A1	240	0.357	1644	1183.68	85.49	0.39	0.00039	8.94E-14
B1	240	0.375	1640	1180.8	85.28	0.79	0.00079	1.51E-12
C1	240	0.358	1644	1183.68	85.49	0.33	0.00033	4.58E-14

Notation	k - Archard Wear coefficient. (m^3/Nm) x10^{15}
A1	2.93
B1	47.1
C1	1.50

The sliding distance can be calculated using the following equation:

$$L = \pi \cdot n \cdot d \tag{3}$$

Where: n – number of revolutions of the driveshaft;
d – ball diameter (mm).
The Archard coefficient can be determined using this equation:

$$k = \frac{\pi b^4}{32 \cdot L \cdot F_N \cdot d} \quad (4)$$

Where: k – Archard coefficient (m^3/Nm);
L – sliding distance (m);
F_N – the ball pressing force (N);
b – imprint diameter(m);
d – diameter of the ball (mm).

4. Conclusions

The concentration of TiB_2 particles influences the properties of the layers and implicitly the value of the Archard coefficient.

It is worth mentioning that the thickness of the external reinforcing layer of the FGMMCs has remained constant throughout the height of the sample.

The dimensional analysis of the samples showed the varying sizes of the dispersed particles from 396.1 nm in diameter to 615.1 nm and a layer size from 1117 µm to 1211 µm.

By mechanical stirring, uniform dimensions are obtained for the TiB_2 particles, the dimensions are varying because of the speed used during the stirring process (200 rpm) with a time of 2 minutes.

The reaction time did not allow the reaction (1) to be completely carried out thus, from the XRD analysis, resulting in intermetallic compounds $TiAl_3$ and $TiAl_2$.

REFERENCES

[1] M. Surappa, “Aluminium matrix composites: Challenges and,” Sadhana, vol. 28, pp. 319-334, 2003.

[2] M. Haghshenas, Metal–Matrix Composites, Waterloo, ON, Canada: University of Waterloo, 2015.

[3] K. Bilge and M. Papila, “Interlayer toughening mechanisms of composite materials,” in Toughening Mechanisms in Composite Materials, vol. 10, Istanbul, Woodhead Publishing Series in Composites Science and Engineering, 2015, pp. 263-294.

[4] A. Bouzekova-Penkova and A. Miteva, “Aluminium-Based Functionally Graded Materials,” Bulgarian Academy of Sciences, vol. 10, 2014.

[5] Z. S. Khodaei, Preliminaries to Modeling and Analysis of Functionally Graded Materials, Prague: Czech Technical University in Prague, Faculty of Civil Engineering, 2005.

[6] A. M. Miteva, “An overview of the functionally graded materials”, Scientific Proceedings II International Scientific-Technical Conference, vol. 14, pp. 71-74, 2014.

[7] J. Yang and H.-S. Shen, “Dynamic response of initially stressed functionally graded rectangular thin plates,” Composite Structures, vol. 54, no. 4, pp. 497-508, 2001.

[8] S. S. Wang, "Fracture mechanics for delamination problems in composite materials," Journal of Composite Materials, vol. 17, no. 3, pp. 210-223, 1983.

[9] T. P. Singh and M. Sahni, "Study of Strength of Rotating Discs of Innovative Composite Material with Variable Thickness," Proceedings of the International multiconference of Engineers and Computer Scientists, vol. 2, 2016.

[10] P. Shanmugavel, G. B. Bhaskar, M. Chandrasekaran, P. S. Man and S. P. Srinivasan, "An overview of fracture analysis in functionally graded materials," European Journal of Scientific Research, vol. 68, no. 3, pp. 412-439, 2012.

[11] A. Saiyathibrahim, R. Subramaniyan and P. Dhanapal, "Centrifugally Cast Functionally Graded Materials – A Review," ICSSCCET, vol. 2, pp. 68-74, 2016.

[12] S. K. Bohidar, R. Sharma and P. R. Mishra, "Functionally Graded Materials: A Critical Review," International Journal of Research, vol. 1, no. 7, p. 289, 2014.

[13] R. M. Mahamood, E. T. Akinlabi, M. Shukla and S. Pityana, "Functionally Graded Material: An Overview," Proceedings of the World Congress on Engineering, vol. III, 2012.

[14] A. Toudehdehghan, J. W. Lim, K. E. Foo, M. Ma'arof and J. Mathews, "A brief review of functionally graded materials," MATEC Web of Conferences, vol. 131, 2017.

[15] Y. Watanabe, Y. Inaguma, H. Sato and E. A. Miura-Fujiwara, "Novel fabrication method for functionally graded materials under centrifugal force: the centrifugal mixed-Powder method," Materials, vol. 2, no. 4, pp. 2510-2525, 2009.

[16] S. Sanaulla and Mr.C.Shashikanth, "Finite Element Analysis of Aluminum Plates with First Order Shear Deformation Theory," International Journal & Magazine of Engineering, Technology, Management and Research, vol. 4, no. 2, pp. 502-510, 2017.

[17] P. Moldovan and M. Buțu, "Tehnici de producere in-situ a materialelor compozite cu aplicații în tehnologia viitorului", Academia de Științe Tehnice din Romania, pp. 204-211, 2013.

[18] A. Monshi, M. R. Foroughi and M. R. Monshi, "Modified Scherrer Equation to Estimate More Accurately Nano-Crystallite Size Using XRD," World Journal of Nano Science and Engineering, vol. 2, pp. 154-160, 2012.

[19] A. Petrescu, A. Tudor, G. Chisiu, N. A. Stoica and U. C. Bayr, "The determination of the thickness of the layers deposited on the electronic circuit boards through tribological methods," IOP Publishing Materials Science and Engineering, vol. 174, 2017.